Eur Biophys J (2000) 28: 639–647

ARTICLE

Sergei P. Rozhkov · Andrei S. Goryunov

Effects of inorganic salts on the structural heterogeneity of serum albumin solutions

Received: 22 December 1998 / Revised version: 23 August 1999 / Accepted: 24 September 1999

Abstract The formation of protein clusters or a protein-rich phase in undersaturated solutions of biopolymers is considered theoretically on the basis of phase diagrams of a water-protein-salt system. Concentrated (50–200 mg/ml of protein) water-salt solutions of human serum albumin molecules modified by a maleimide spin-label have been studied experimentally using the ESR technique to characterize the significant general features of the system behaviour suggested by the model phase diagrams. The inorganic ion content (NaCl, KSCN, $MgCl_2$, and $CaCl_2$) was varied in the range of 10^{-3}–4 M. Salt-induced changes in different experimental ESR spin-label parameters based on relations between spectral line widths and amplitudes were determined and compared with the same parameters in salt-free solution. The data on dipole-dipole interactions of spin labels obtained at 77 K and on spin exchange at normal temperatures are indicative of local protein concentration inhomogeneities. The results have been described in terms of salt-induced dissociation of stabilized supramolecular structures in protein solution–protein clusters, liquid-liquid phase transition between the hydration water of clusters and that of individual proteins, and a rise in surface tension which results in protein stabilization.

Key words Protein clusters · Phase diagrams · Protein-salt interaction · Protein hydration · ESR spin labeling

Introduction

Being one of the levels of supramolecular organization, the dynamical (reversible) self-association and aggregation of dissolved macromolecules is biologically and medically significant (De Young et al. 1993). There is increasing evidence obtained by precise physical methods that, under certain conditions, globular protein molecules can build up clusters (Giordano et al. 1991; Petit et al. 1997), different oligomers (Verheul et al. 1999) or microcoacervates, i.e. protein-rich microphases in a protein-lean phase (Miyakawa et al. 1995), even in diluted solutions, whose structural organization is thus revealed. There are processes likely to be connected with binary liquid-liquid phase separation (for refs., see De Young et al. 1993; Miyakawa et al. 1995), rather than with nucleation of a new phase leading to amorphous precipitation of protein or its crystallization in supersaturated solutions. Hence, protein clusters are assumed to be long-lived stabilized fluctuations of protein concentration and they may be thought of as the nuclei of a "hidden" phase (Askhabov and Ryazanov 1998).

Ordered structures arise usually because of peculiar interaction between particles with potential that exhibits a secondary minimum. The ordering of protein solutions is described sometimes within the framework of Deryagin-Landau-Verwey-Overbeek (DLVO) theory (De Young et al. 1993; Israelachvili and Wennerstrom 1996). DLVO and related theories can account for the electrostatic energy of repulsion and molecular energy of attraction between particles in solution. However, not much can be suggested on the reasons for stability of protein solutions in the presence of moderate and high salt concentrations. Some progress, made recently in this field, is related to the addition of the structural component of disjoining pressure to the energy of interaction of weakly charged hydrophilic surfaces (Ovcharenko et al. 1987). In water solutions, this contribution gives rise to hydration forces (Rand 1992; Israelachvili and Wennerstrom 1996) which can affect protein aggregation.

Using the ESR method, the phase transition from the "low-salt" to "high-salt" structure of solutions has been shown to occur in the range of physiological NaCl concentrations far below the "salting-out" range,

S.P. Rozhkov · A.S. Goryunov (✉)
Institute of Biology, Karelian Research Centre,
Russian Academy of Sciences, Pushkinskaya 11,
185610 Petrozavodsk, Russia
e-mail: goryunov@post.krc.karelia.ru

accompanied by the alteration of surface tension in the water-protein matrix of serum albumin molecules (Rozhkov 1992, 1996, 1997; Rozhkov and Borisova 1993). In this work we study the effects of different inorganic salts on the water-protein matrix of serum albumin molecules in the process of transformation of water (1)-protein (2)-salt (3) solutions from "low-salt" to "high-salt" structures using ESR spin-labelling and low-temperature ^{1}H NMR methods, and discuss this process in terms of salt-induced dissociation of protein clusters. Another goal of this work is to qualitatively describe a phase diagram for pseudo-three-component (water-protein-inorganic salt) solutions in order to characterize its structural organization and phase transitions over a wide range of concentrations of all the components.

Materials and methods

Lypophilized human serum albumin (HSA) preparations (Reanal) were dissolved in distilled water, pH 5.8. To modify the HSA molecule, we used the spin label *N*-(1-oxyl-2,2,6,6-tetramethylpiperid-4-yl)maleimide (Reanal) in dioxane. The mixture of protein with a fivefold molar excess of the label (for a dioxane content <3%) was incubated for 12 h at 4 °C. The solution of modified (spin-labelled) albumin (HSA-SL) was purified on a G-200 column, using 0.001 M phosphate buffer, pH 7.3, or 0.01 acetate buffer, pH 6.4, as eluate. The fraction of HSA-SL monomers was concentrated to 220–250 mg/ml and used as stock solution. The protein concentration was controlled spectrophotometrically ($\lambda = 280$ nm, $D^{1\%}_{1cm} = 5.8$). All the salts used were reagent grade. The required salt concentration in the protein solutions was obtained by adding equal volumes of the salt solutions of the corresponding weighed batches in appropriate buffer. NaCl solutions were made in 0.001 M phosphate buffer. $CaCl_2$, $MgCl_2$ and KSCN solutions were made in 0.01 M acetate buffer.

In the case of $CaCl_2$ and $MgCl_2$, effective interaction of cations with the protein (Arakawa and Timasheff 1984) leads to a decrease in the pH values of the solution. Allowance has been made for salt-induced changes in pH in order to obtain data under the same conditions. Measurements were performed in protein-$CaCl_2$ or -$MgCl_2$ solutions and in salt-free solutions with the pH adjusted to its value in the presence of the salts. The pH of the solution was changed by adding HCl.

The ESR spectra of HSA-SL were recorded with a RE-1306 radiospectrometer, 9.4 GHz, 100 kHz field modulation. The sample temperature was regulated to ± 0.5 K with a thermostated resonator unit. Temperature dependences were measured by heating from 5 to 25 °C with steps of 2–4 °C. The samples were held at a given temperature for 7–10 min before taking the spectrum. The experimental parameters used in the analysis of the ESR spectra are shown in Fig. 1.

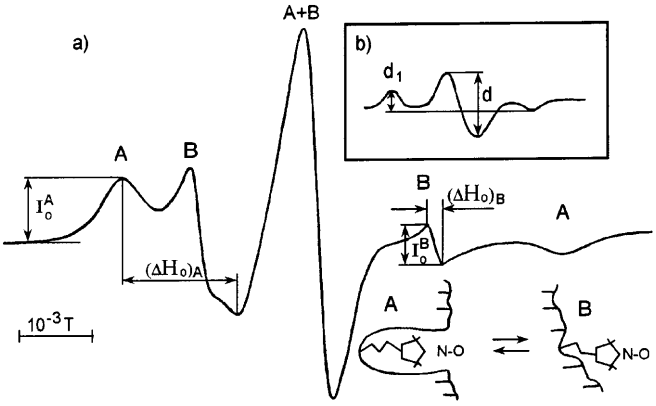

Fig. 1a, b ESR Spectrum of spin-labelled HSA-SL macromolecules. **a** Protein concentration 36 mg/ml, 0.01 M phosphate buffer, pH 7.3, 0.15 M NaCl, temperature 20 °C. The symbols *A* and *B* indicate the positions of the spectral components, corresponding to the strong and weak immobilization of spin label. I_0^A, $(\Delta H_0)_A$ and I_0^B, $(\Delta H_0)_B$ show the experimental parameters used for calculation of an effective label distribution between *A* and *B* states. **b** Temperature 77 K. d_1 is the sum of the amplitudes of the low-field and high-field spectral lines and d is the amplitude of the central component of the spectrum. The ratio d_1/d is used to estimate an average interprotein distance

Two ESR spectral components corresponding to strong (A) and weak (B) immobilization of the label are observed (Fig. 1a). In HSA solution of pH $\approx$ 6, maleimide spin-label reacts solely with the SH group of Cys34 located in the protein surface crevice about 1 nm deep, which configuration is not rigid and undergoes thermal transitions between states differing in the mobility of spin label (Wetzel et al. 1980). The number of SH groups labelled (0.6 mol/mol protein) was determined by double integration of the ESR spectra of the sample and the standard at 77 K.

The experimental parameter d_1/d determined at 77 K (see Fig. 1b) was employed as a measure of the intensity of the dipole-dipole interaction of spin labels caused by changing the local concentration of spin-labelled macromolecules (Likhtenstein 1974; Wasserman and Kovarskii 1986). To this end, samples of HSA-SL solutions of different salt concentrations in cuvettes were conditioned at 5 °C for several hours and then immersed immediately in liquid nitrogen.

The spectral subtraction technique is sometimes used to measure the concentration ratio of A and B states to study this conformational transition in detail (Graceffa and Lehrer 1984). The goal of this ESR spin-label experiment is to find tendencies in salt-induced changes of solution structure, the $A \rightleftharpoons B$ equilibrium being an indicator of a salt effect. To this end, an effective value of $K^{ef} \approx [A]^{ef}/[B]^{ef}$ can be used, where $[A]^{ef}$ and $[B]^{ef}$ are the effective spin concentrations obtainable from spectral parameters. The $A \rightleftharpoons B$ equilibrium constant K depends on the spectral parameters according to the following expression.

$$K = k_1 I_0^A (\Delta H_0)_A^2 / k_2 I_0^B (\Delta H_0)_B^2 \quad (1)$$

where k_1 and k_2 are the constants depending on the spectrum lineshape for A and B components, respectively. Although the spectral linewidth cannot give the true value of $(\Delta H_0)_A$ in the case of slow diffusion of the spin label, we have found experimentally that the effect of variations of the linewidth ratio of A and B spectral components $(\Delta H_0)_A^2/(\Delta H_0)_B^2$ on the value of K is negligible compared with the effect on this value of variations of the amplitude ratio I_0^A/I_0^B. The shape of the spectra does not change dramatically within the 5–25 °C temperature range and at the salt concentrations studied. On this basis we consider the ratio k_1/k_2 to be constant factors of K, whereas the changes in K are substantially due to the changes in the I_0^A/I_0^B ratio throughout the salt concentration range covered. Hence, we used the van't Hoff plots of the parameter

$$K^{ef} = I_0^A(\Delta H_0)_A^2/I_0^B(\Delta H_0)_B^2 \quad (2)$$

to estimate salt-induced *changes* in the equilibrium values of the enthalpy $\Delta H^{ef} = \Delta H_A - \Delta H_B$, the entropy $\Delta S^{ef} = \Delta S_A - \Delta S_B$ and the free energy $\Delta G^{ef} = \Delta G_A - \Delta G_B$.

Protein hydration was studied using the Kuntz methodology for determining non-freezing water by low-temperature ^{1}H NMR. Absolute hydration values were calculated, using a signal of the standard (24% LiCl, 0.10% $MnCl_2$ aqueous solution), which remains non-freezing up to −50 °C and has a water concentration of 48.5 M at −35 °C (Hays and Fennema 1982). The integral intensity of the resonant water protons absorption band was registered, using a Tesla BS-467 (60 MHz) ^{1}H NMR spectrometer equipped with a standard thermostatic unit with a temperature maintenance accuracy of ± 1 °C.

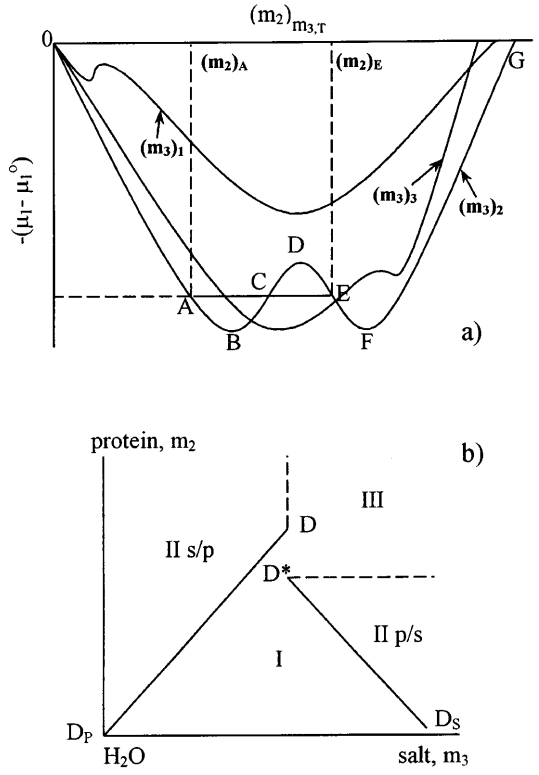

Fig. 2a, b Two forms of phase diagrams of water-protein-salt solutions. **a** Chemical potential of water $\mu_1 - \mu_1^\circ$ versus protein concentration m_2 at constant salt concentration m_3. The form of the isothermal dependence changes with m_3 (indicated by *arrows*) in the salt concentration range: $(m_3)_1 < (m_3)_2 < (m_3)_3$. $A \rightleftharpoons E$ is the metastable state of two liquid phases; $(m_2)_E$ is protein concentration in cluster, $(m_2)_A$ is concentration of monomers in solution. **b** Protein concentration m_2 versus salt concentration m_3. D_pD and D_sD^* are critical transition lines. See text for details

Theory

The behaviour of the water-protein-salt system on changing the relative concentrations of its components can be considered on the basis of phase diagrams. The coexistence of macromolecules and their clusters requires at least the equality of the chemical potentials of water in the hydration shell of a macromolecule and in the hydration shell of a cluster. The simplest type of phase diagram for a multi-component system [water (1)-protein (2)-salt (3)] is a plot of chemical potential of water $\mu_1 - \mu_1^\circ$ against protein concentration m_2 with salt concentration m_3 used as a parameter (Arakawa and Timasheff 1982). A "van der Waals loop" is to be expected on the phase isotherm (Fig. 2a) for a colloid dispersion that contains interacting particles (Belousova and Buevich 1988) and particularly for a water-protein-salt system (Rozhkov 1988, 1996). When the protein concentration reaches the $(m_2)_B$ value, instability arises and spinodal decomposition begins (Binder 1981). This diffusion-limited process is poorly investigated in protein solutions as yet. It probably brings about the establishment of the metastable state $A \rightleftharpoons E$, where $(m_2)_E$ and $(m_2)_A$ are protein concentrations in clusters and in their environment, respectively. The metastability of the $A \rightleftharpoons E$ state in Fig. 2a suggests the equality of chemical potentials of water in clusters and in solutions of protein monomers.

A critical protein concentration is reached at the point $(m_2)_D$. The metastable state $A \rightleftharpoons E$ is not established here since monomolecular and cluster solution organizations are readily interconverted owing to the low activation energy of association and do not coexist. The position of the critical point in Fig. 2a (or critical line in coordinates $[m_2, m_3]$) is determined as (Rozhkov 1988, 1996):

$$(m_2/m_3)_{cr} \approx \frac{4}{v(2-B)}\left\{1 + \left(1 + \frac{(2-B)^2}{z^2}v^2\right)^{1/2}\right\} \quad (3)$$

where v is the number of ions adsorbed on the protein surface at specific binding sites, z is the protein charge, and B is the temperature-dependent parameter responsible for an alteration of water activity in the salt solution. It follows from Eq. (3) that the critical state of the

solution can be approached by changing the protein concentration at a given salt concentration or by changing the salt concentration at a given protein concentration. Phase isotherms in coordinates (μ_1, m_2) may look like phase isotherms in coordinates (μ_1, m_3).

A combination of these two pairs of coordinates yields a new type of phase diagram (Fig. 2b). The segment of molecular solubility is marked I on the phase diagram. The label III marks the section where the salt and protein crystalline phases may coexist in equilibrium with the saturated solution of these components. A low-salt zone marked IIs/p can represent a colloid two-phase system of a water-protein mesophase (probably, diffusion limited cluster-cluster association) as a disperse medium and the water-salt solution as a disperse phase. The two-phase system labeled IIp/s (high salt content) represents the concentrated water-salt solution as a disperse medium with partly dehydrated "salted out" protein aggregates as a disperse phase. All these phases are linked to zone DD*. A salt-free solution of serum albumin was shown to form a fractal structure through diffusion-limited cluster-cluster association (Magazy et al. 1989). Accordingly, "salting in" can represent the destruction of the clusters. One of the stages of this transition is a monomer-cluster metastable state formed in the zone adjacent to the critical line D_pD, whereas protein aggregates (precipitates) are formed in the zone adjacent to the critical line D_sD^*. Hence, DD* is a zone where protein clusters, aggregates, microcrystals and monomers may arise from large fluctuations of concentration in a "microemulsion" state, but these types of associates cannot coexist in equilibrium.

The phase diagram in Fig. 2b that resembles the dependence of protein solubility against ionic strength can predict qualitatively the rise of different solution structures and transitions between them. The results presented in the following sections were obtained to generally characterize some significant features of system behaviour.

Results

Salt-induced changes of spin-label dipole-dipole interaction

The dependence of the experimental parameter d_1/d on salt concentration is shown in Fig. 3. At a concentration of spin labels less than or equal to 7×10^{-3} M, dipole-dipole interaction between them does not show up in ESR spectra (Wasserman and Kovarskii 1986) and the value of d_1/d is about 0.4 (Likhtenstein 1974). The concentrations of single spin-labelled proteins in Fig. 3 are much lower. Therefore, the rise of d_1/d over 0.4 with decreasing salt concentration is indicative of the intensive dipole-dipole interaction and thus of local concentration inhomogeneities of protein molecules (clusters, aggregates). The dependence of d_1/d on solution composition characterizes the change in the inhomogeneities. It follows from Fig. 3 that within moderate $CaCl_2$, $MgCl_2$ and NaCl concentration ranges (0.05–1.3 M) the local concentration of HSA-SL is lowered as d_1/d is decreased. In accordance with the calibration curve, which gives the dependence of d_1/d (Likhtenstein 1974), the average distance between paramagnetic sites increases by 2.0–2.5 nm.

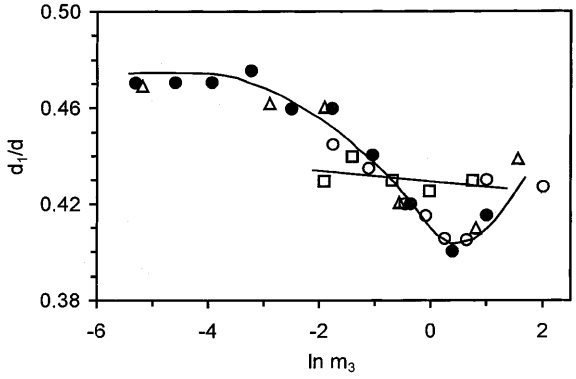

Fig. 3 Parameter d_1/d of ESR spectra versus salt concentration. $CaCl_2$, HSA-SL concentration 110 mg/ml, pH 6.4 (●); $MgCl_2$, HSA-SL concentration 90 mg/ml, pH 5.7 (○); NaCl, HSA-SL concentration 40 mg/ml, pH 7.3 (△); KSCN, HSA-SL concentration 110 mg/ml, pH 6.4 (□). Temperature 77 K. *Solid curve* is drawn for data of $CaCl_2$, $MgCl_2$ and NaCl concentration dependences to guide the eye. *Straight line* is for KSCN

The properties of the solution change on lowering the temperature to 77 K as well as the balance of ion-electrostatic, hydration and molecular forces that stabilize the volume distribution of spin-labelled macromolecules. Nevertheless, the general characteristics of this distribution persist owing to the fast freezing of samples and the strongly diffusion-limited type of formation of protein concentration inhomogeneities. It is very unlikely that the uneven distribution of protein molecules in solution, which takes from several tens of minutes to hours to be established (Giordano et al. 1991), can be noticeably shifted to a new state during a fraction of a second of freezing in the capillaries. On this basis, the data presented in Fig. 3 suggest the concentration inhomogeneities in the protein solution at normal temperatures as well, and this is supported by the following results.

Salt induced changes of spin-label diffusion and spin exchange

The correlation time τ_c was calculated formally, using an equation for an isotropic model of spin-label motion (Berliner 1976): $\tau_c = 2.55 \times 10^{-9} \ (1 - 2A'_{zz}/A_{zz})^{-0.615}$, where $2A'_{zz}$ is the distance between the low-field and the high-field lines of immobilized spectrum A components, and $2A_{zz}$ is that for 77 K, when rotation of label N-O group is frozen. These data are presented in Fig. 4 against salt concentration. It is seen that τ_c rises within a

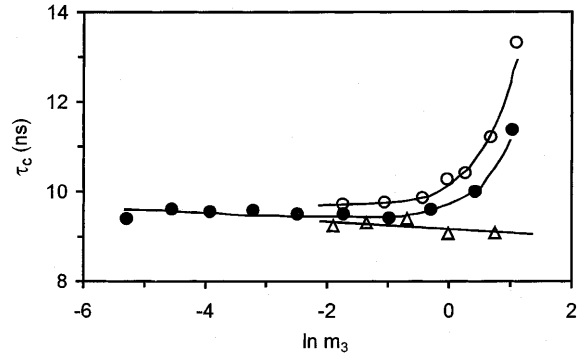

Fig. 4 Rotation correlation time τ_c of the spin label versus salt concentration. $CaCl_2$, HSA-SL concentration 110 mg/ml, pH 6.4 (●); $MgCl_2$, HSA-SL concentration 90 mg/ml, pH 5.7 (○); KSCN, HSA-SL concentration 110 mg/ml, pH 6.4 (△). Temperature 10 °C

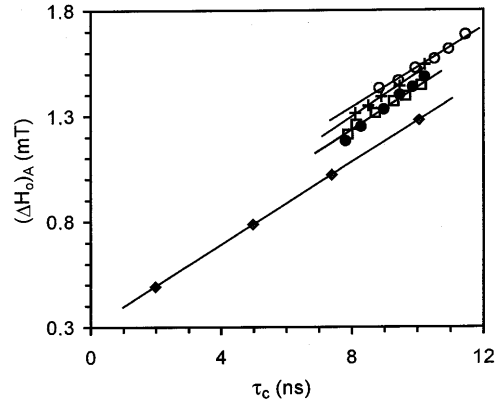

Fig. 5 Parameter $(\Delta H_0)_A$ versus rotation correlation time τ_c of spin label. HSA-SL concentration 50 mg/ml, pH 7.3, 0.15 M NaCl (●); 2 M NaCl (+); 4 M NaCl (○); no NaCl (□); dependence of $(\Delta H_0)_A$ on τ_c for the model spectrum of non-solvated label with a standard set of magnet interaction constants (Antsiferova et al. 1977) (◆). τ_c values were varied by changing the temperature from 5 to 25 °C

high salt concentration range. This is probably a result of salt-induced protein stabilization (Arakawa and Timasheff 1982) that brings about an increase of microviscosity in the cavity of the spin-label location.

Model spectra for isotropic label diffusion with different τ_c (Antsiferova et al. 1977) show that the experimental parameter $(\Delta H_0)_A$ approaches the intrinsic linewidth X when label diffusion increases. $(\Delta H_0)_A$ values at high τ_c are characteristic mostly of a label diffusion in the water-protein matrix. It is seen in Fig. 5 that the dependence of the width of $(\Delta H_0)_A$ on correlation time τ_c follows the expression:

$$(\Delta H_0)_A \approx \alpha\tau_c + X + \Delta X \quad (4)$$

where α varies with hyperfine constant A_0 which is increased when the radical is solvated by polar solvent, X is the intrinsic line width ($X = 0.3$ mT) and ΔX is the additional broadening of the line depending on the interaction of the spin labels at the diffusing proteins. Such interaction can significantly affect the ESR lineshape under conditions of this experiment and at room

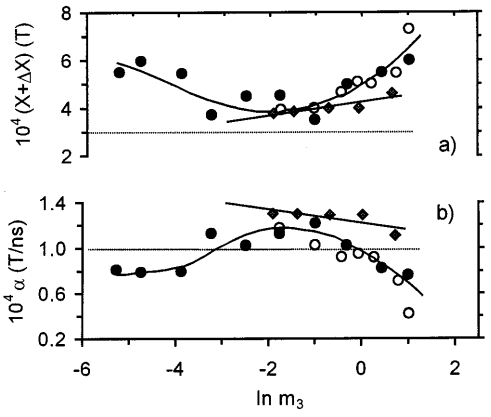

Fig. 6 Parameters $X + \Delta X$ and α versus salt concentration. $CaCl_2$, HSA-SL concentration 110 mg/ml, pH 6.4 (●); $MgCl_2$, HSA-SL concentration 90 mg/ml, pH 5.7 (○); KSCN, HSA-SL concentration 110 mg/ml, pH 6.4 (◆). *Solid lines* are drawn to guide the eye. *Dotted line* indicates the theoretical α and X values of non-solvated spin label with a standard set of magnet interaction constants (Antsiferova et al. 1977)

temperatures only in the case where the frequency of spin-spin contacts is considerably enhanced. This can occur when spin-labelled macromolecules are clustered or aggregated. In concentrated NaCl solutions, $(\Delta H_0)_A$ and ΔX increase (Fig. 5), indicating the intensification of the labels spin-spin exchange at "salting-out" concentrations. Therefore, in parallel with a decline in label diffusion due to protein stabilization (Fig. 4) there occurs a rise in the frequency of the spin-spin contacts. This is likely to be due to protein aggregation. The amplitude of the HSA-SL spectrum in concentrated salt solution decreases with rising temperature, also suggesting the intensification of spin exchange.

Experimental values of $X + \Delta X$ and α for solutions containing $CaCl_2$, $MgCl_2$ and KSCN are shown against salt concentration in Fig. 6. The increased ΔX in water-protein solutions of low salt concentration indicates concentration inhomogeneities. The amount of the latter decreases with rising salt concentration. At the same time, values of α (Fig. 6b) in high and low salt concentrations are smaller than those theoretically estimated from model spectra for a dehydrated radical with a standard set of magnetic parameters [theoretical values of α (Fig. 5 and Antsiferova et al. 1977) are shown by a dotted line in Fig. 6b]. This presumably is the result of the more intensive widening of the B-component owing to the spin exchange compared with the narrowing of the A-component owing to the thermo-induced increase of the label diffusion.

Thermodynamic approach to the analysis of HSA-SL spectra

ΔH^{ef}, ΔS^{ef} and ΔG^{ef} values, calculated from van't Hoff plots using Eq. (2), are presented in Fig. 7 against

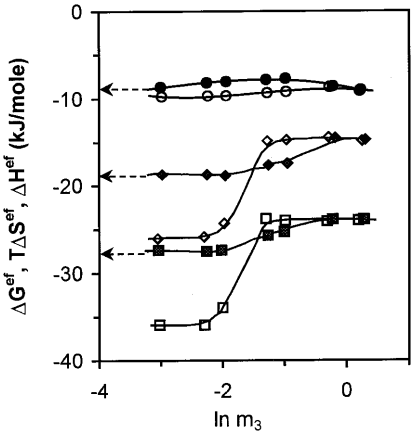

Fig. 7 Thermodynamic parameters versus NaCl concentration. ΔG^{ef} (●, ○), $T\Delta S^{ef}$ (◆, ◇) and ΔH^{ef} (■, □); HSA-SL concentration is 50 mg/ml (●, ◆, ■) and 200 mg/ml (○, ◇, □); pH 7.3. The values of the parameters are reduced to 10 °C

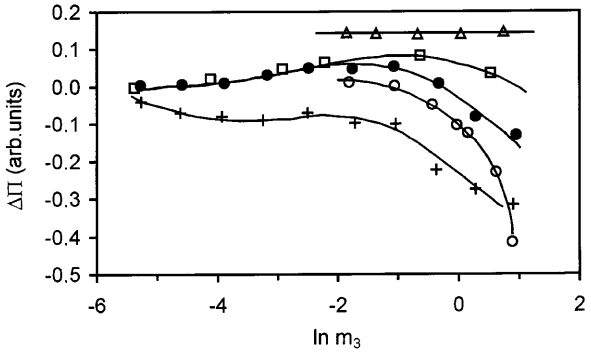

Fig. 8 Relative parameter $\Delta\Pi$ versus salt concentration m_3. $CaCl_2$, HSA-SL concentration 110 mg/ml, pH 6.4 (●); $MgCl_2$, HSA-SL concentration 90 mg/ml, pH 5.7 (○); NaCl, HSA-SL concentration 200 mg/ml, pH 7.3 (□); KSCN, HSA-SL concentration 110 mg/ml, pH 6.4 (△); $CaCl_2$, HSA-SL concentration 110 mg/ml, allowance is made for salt-induced changes in pH (+)

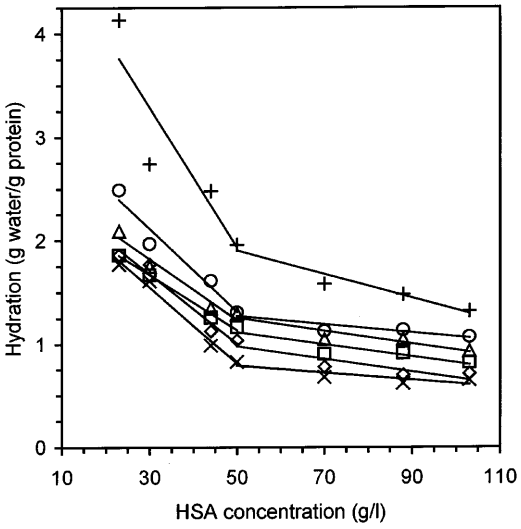

Fig. 9 Protein hydration versus HSA concentration. 0.01 M phosphate buffer, pH 7.3, 0.15 M NaCl, temperatures are as follows: −10 °C (+), −15 °C (○), −20 °C (△), −25 °C; (□), −30 °C (◇), −35 °C (×)

NaCl concentration. Similar curves were obtained for $CaCl_2$ and $MgCl_2$ (not shown). The difference was that at higher $CaCl_2$ or $MgCl_2$ concentrations, ΔH^{ef} and ΔS^{ef} decreased again. KSCN did not cause any changes in ΔH^{ef} and ΔS^{ef} within the experimental error in the concentration range of Fig. 7. The curves show the difference in equilibrium parameters of A and B states of the label at low and moderate salt concentrations. Furthermore, the higher the protein content, the greater the amplitude of the change of ΔH^{ef} and ΔS^{ef}. Essentially negative values of enthalpy and entropy at low salt concentration can be due to highly ordered hydrogen-bonded water structures in the water-protein matrix. As the salt concentration rises, this water structure "melts" (phase transition) and transforms into a structure characteristic of liquid water with higher but yet negative ΔH^{ef} and ΔS^{ef} values.

Despite the plainly marked compensating entropy-enthalpy effect, the specific extreme of the dependence of ΔG^{ef} on NaCl, $MgCl_2$ and $CaCl_2$ concentration is evident. This extreme is more pronounced when the data are presented in the form of the dependence of the relative parameter $\Delta\Pi = (\Delta G_2^{ef} - \Delta G_1^{ef}/|\Delta G_1^{ef}|$ on salt concentration, shown in Fig. 8. Here ΔG_1^{ef} is the free energy difference of the label A and B states in salt-free solution and ΔG_2^{ef} is that in the presence of salt in solution. The negative sign of $\Delta\Pi$ (high salt concentrations) indicates that the A state of the label is more preferable (the B state is less preferable) at a given salt concentration in comparison with salt-free solution. A positive $\Delta\Pi$ is suggestive of an enhancement of the spin-label interaction with the solvent, i.e. the "open" B state is more populated.

The lower curve in Fig. 8 shows the tendency of $\Delta\Pi$ changes, with allowance made for salt-induced changes in pH. It is seen that in this case there is a negative shift of $\Delta\Pi$ in all the $CaCl_2$ concentration range, with a plateau at moderate salt concentrations.

Changes in protein hydration

The concentration dependence of HSA hydration has two approximately linear segments of different negative slopes at all the temperatures studied (Fig. 9). The transition point between the segments is at about 50 mg/ml or 200 M NaCl per 1 M protein. The values of hydration at the steeper segment are high compared with those previously obtained by various techniques for ion-free solutions (Rupley and Carreri 1991). HSA hydration in the salt-free solution at 48 mg/ml concentration was 0.2 g/g, which is quite normal.

Discussion

Experimental data (Figs. 3–8) can be considered as reflecting the path of the system of constant protein

concentration on the phase diagram when salt concentration changes. The mesophase state of the protein solution in the low salt concentration range (IIs/p) (Fig. 2b) emerges as the protein concentration inhomogeneities (elevated values of d_1/d in Fig. 3 and ΔX in Fig. 6). The water-protein matrix of HSA-SL shows a very orderly pattern characterized by large negative ΔH^{ef} and ΔS^{ef} (Fig. 7).

On approaching the critical line D_pD in the moderate salt concentration range, the "low-salt" structure of the solution and the water-protein matrix "melts" (the values of entropy and enthalpy in Fig. 7 become less negative). "Melting" is accompanied by a decrease of protein concentration inhomogeneity (d_1/d in Fig. 3 and ΔX in Fig. 6 decrease). Positive values of $\Delta\Pi$ in Fig. 8 indicate that the water-protein matrix is destabilized (the B state of the label is more preferable since ΔG_2^{ef} is less negative) and becomes more accessible for solvent in this salt concentration range than is the case in salt-free and high-salt solutions.

When passing the critical line D_pD, the concomitant shift of phase state from clusters to individual molecules manifest itself in a sleep rise in protein hydration (Fig. 9) as the m_3/m_2 value increase because (1) the specific sites, inaccessible for ions in the interior of a protein cluster, form highly hydrated centres with ions penetrating the water-protein matrix of individual (non-cluster) molecules, (2) protein hydration on a per macromolecule basis is greater for an individual molecule compared to that for a molecule in a cluster.

In the vicinity of the critical line D_sD^*, where protein clusters dissociate, the process is strongly influenced by the factor of "preferential hydration" (Arakawa and Timasheff 1984; Arakawa et al. 1990). Non-bound ions are excluded from the protein hydration shell, which leads to protein stabilization under "salting-out" conditions (Fig. 4 and Arakawa and Timasheff 1984). The water surface tension increment $d\sigma/dm_3$ of all the salts used is positive but different: $CaCl_2 > MgCl_2 > NaCl \gg$ KSCN (Arakawa and Timasheff 1984). The free energy $\Delta\mu_2$ of transfer of proteins from an aqueous to a salt medium is also positive since $(\partial\mu_2/\partial\mu_3)_{m2} = N_A S_2 (\partial\sigma/\partial m_3)_{m2}$, where S_2 is the surface area of the protein molecule. The thermodynamically unfavourable increase of μ_2 caused by a surface tension rise may be compensated by a decrease of S_2, resulting in protein stabilization. The relative parameter $\Delta\Pi$ must be sensitive to the surface tension in the spin-label cavity as it reflects changes in the free energy of the label A and B states. The elevation of negative $\Delta\Pi$ (Fig. 8) reflecting stabilization of the label A state suggests the stabilizing effect of Ca^{2+} and Mg^{2+} on a protein molecule at high salt concentrations.

The thermodynamically metastable state $A \rightleftharpoons E$ is most probably a kinetically stabilized state. The colloid dispersion particles that are large compared to the molecular size are known to be thermodynamically unfavourable because of increased surface energy and decreased entropy. On the other hand, the formation of an electrical double layer (EDL) around protein clusters tends to increase the entropy and decrease the surface tension (Frolov 1987), thus compensating the free energy rise. In the vicinity of the hydrophilic surface, EDL universally arises when the cation and anion radii of hydration differ, regardless of the presence of surface charges (Dukhin and Yaroshchuk 1982). This gives rise to an effective ion-electrostatic energy of repulsion between clusters, whereas the hydration shells of clusters contribute crucially to the hydration forces of repulsion. The combination of these components of energy with the molecular energy of attraction determines the potential curves. An increase of electrolyte concentration causes regulation of amplitude and position of potential barriers, leading to their reduction. The state $A \rightleftharpoons E$ is thus destabilized. When the number of salt ions is enhanced and the ratio $(m_3/m_2)_{cr}$ is exceeded, the macromolecules surrounded by the ion atmosphere diffuse indpendently. This is evident from the rise of entropy of the system. Such a state of protein solution experimentally manifests itself as a maximum decrease in protein concentration inhomogeneity (decrease of d_1/d parameter in Fig. 3 and ΔX in Fig. 6).

The characteristic extreme of ΔG^{ef} (Fig. 7) following the steep rise in ΔH^{ef} and ΔS^{ef} coincides with the extreme $\Delta\Pi$ in Fig. 8 and indicates a critical-type phase transition which is the limiting case of water-protein matrix "melting" (Rozhkov and Borisova 1993). Hence, one can estimate $(m_2/m_3)_{cr}$ using the salt concentration at positive $\Delta\Pi$ extremes. As follows from Fig. 8, $(m_2/m_3)_{cr}$ reaches 200–250 ions per protein for NaCl, 150–200 ions per protein for $CaCl_2$ and probably far less for KSCN. This is greater than the number of specific combining sites per protein (v) (Record et al. 1978), which to a first approximation varies inversely with $(m_2/m_3)_{cr}$ [Eq. (3)]. These effective values are likely to depend on the penetrating capability (solubility) of different kinds of ions in the hydration shell of the protein to a greater extent than on the number of combining sites. Enhanced dissolving capacity for any component of two liquid phases is known for a critical state. Therefore, in a critical state of hydration water, salt ions will be included into the water-protein matrix and interact with the binding sites of the protein interior.

At the same ion to protein molar ratio, a transition in the concentration dependence of protein hydration (Fig. 9) is observed. Lowering of the hydration with protein concentration is known to be caused by protein association (Cavatorta et al. 1976; Gasan et al. 1994). However, a two-stage decrease in hydration has not been reported for ion-free solutions. Thus, the steeper segment (Fig. 9) is likely to result from protein-ion interaction, namely, a transition from a non-contact type at higher HSA concentration to a contact type at high ion-protein ratios. It is significant that cluster dissociation must be accompanied by a critical-type phase transition between two pseudophases of hydration shells, i.e. water, associated with protein clusters and water associated with proteins.

In addition, ions in solution can generate osmotic forces which destroy the hydration barrier that prevents protein aggregation. In the high-salt concentrations range, when the Debye length is small and hydration barriers also vanish, the molecular forces of attraction are crucial. A large positive surface tension increment leads to the rise of surface free energy μ_2 and to aggregation of the macromolecules. This can result in an increase of the rotation correlation time of the spin label (Fig. 4), which reflects the structural rigidity of the water-protein matrix, and intrinsic spectral line width ΔX (Fig. 6). On the other hand, Mg^{2+} and Ca^{2+} ions at high concentrations are known to be intensively bound to the protein surface (Arakawa and Timasheff 1984; Arakawa et al. 1990) and give rise to strong short-range repulsive forces that prevent aggregation. These hydration forces can result from the residual hydration shells of bound cations (Pashley and Israelachvili 1984). The divalent cations are strongly hydrated and, therefore, do not easily shed their hydration layers in order to bind to the surface. A Mg^{2+} ion is more effective than a Ca^{2+} ion because of its smaller size and a greater polarizing field. The formation of a new hydration barrier prevents protein aggregation and precipitation, and is responsible for the ''salting-in'' properties of these salts at high concentrations.

Conclusions

The analysis of the model phase diagrams and some experimental results presented on the effect of salt on the dynamics of spin-label rotation in the water-protein matrix of HSA-SL indicate that phase transition from ''low-salt'' to ''high-salt'' structure occurs in the water-protein matrix and in water-protein-salt solution as a whole. The system passes through a metastable (protein monomer-protein cluster) state in the moderate salt concentration range. The interaction of the protein binding sites with ions that initially poorly penetrate the protein interior owing to the low dissolving capacity of boundary water intensifies during the phase transition. Hydrated ions saturate the water-protein matrix with water molecules which ''disjoin'' the crevices of the protein interior. Hence, the collective behaviour of protein molecules, caused by long-range forces, may be of great importance in the regulation of the protein dynamic structure.

Although our analysis is speculative, the results indicate that the experimental data obtained within the protein and salt concentration range studied cannot be considered regardless of protein solution heterogeneity.

References

Antsiferova LI, Wasserman AM, Ivanova AN, Livshits VA, Nazemets NS (1977) Atlas of spectra of electron paramagnetic resonance of spin labels and probes. Nauka, Moscow

Arakawa T, Timasheff SN (1982) Preferential interactions of proteins with salts in concentrated solutions. Biochemistry 21: 6545–6552

Arakawa T, Timasheff SN (1984) Mechanism of protein salting in and salting out by divalent cation salts: balance between hydration and salt binding. Biochemistry 23: 5912–5923

Arakawa T, Bhat R, Timasheff SN (1990) Preferential interactions determine protein solubility in three-component solutions: the $MgCl_2$ system. Biochemistry 29: 1914–1923

Askhabov AM, Ryazanov MA (1998) Clusters of ''hidden'' phase–quatarones and nucleation. Dokl Akad Nauk 362: 630–633

Belousova OA, Buevich YuA (1988) Equilibrium properties of the uniform colloid system. Russ Colloid J 50: 217–223

Berliner LJ (ed) (1976) Spin labelling. Theory and application. Academic Press, New York

Binder K (1981) Kinetics of phase separation. In: Arnold L, Lefever R (eds) Stochastic nonlinear systems in physics, chemistry, and biology. Springer, Berlin Heidelberg New York, pp 62–71

Cavatorta F, Fontana MP, Velci A (1976) Raman spectroscopy of protein-water interactions in aqueous solutions. J Chem Phys 65: 3635–3640

De Young LR, Fink AL, Dill KA (1993) Aggregation of globular proteins. Acc Chem Res 26: 614–620

Dukhin SS, Yaroshchuk AE (1982) Problem of the boundary layer and the electrical double layer Kolloidn Zh 44: 884–894

Frolov YuG (1987) The basic relationships of the thermodynamic theory of the aggregative stability of disperse systems. Russ Colloid J 49: 93–97

Gasan AI, Kashpur VA, Maleev VYa (1994) thermal rearrangements and hydration of serum albumin. Biophysics 39: 588–593

Giordano R, Grasso A, Wanderlingh F, Wanderlingh U (1991) Static and dynamic properties in thixotropic structures. Prog Colloid Polym Sci 84: 487–493

Graceffa P, Lehrer SS (1984) Dynamic equilibrium between the two conformational states of spin-labeled tropomyosin. Biochemistry 23: 2606–2612

Hays DI, Fennema O (1982) Methodology for determining of unfreezable water in protein suspensions by low temperature NMR. Arch Biochem Biophys 213: 1–6

Israelachvili J, Wennerstrom H (1996) Role of hydration and water structure in biological and colloidal interactions. Nature 379: 219–225

Likhtenstein GI (1974) Method of spin labels in molecular biology. Nauka, Moscow

Magazy S, Maisano G, Mallamace N, Micali N (1989) Growth of fractal aggregates in water solutions of macromolecules by light-scattering. Phys Rev A 39: 4195–4200

Miyakawa K, Totoki M, Kaibara K (1995) Effects of metal cations on coacervation of alpha-Elastin. Biopolymers 35:85–92

Ovcharenko FD, Estrella-Liopis VR, Dudnik VV (1987) The new type of potential curves for lyophilic systems. Dokl Akad Nauk SSSR 293: 660–665

Pashley RM, Israelachvili JN (1984) DLVO and hydration forces between mica surfaces in Mg^{2+}, Ca^{2+}, Sr^{2+}, and Ba^{2+} chloride solutions. J Colloid Interface Sci 97: 446–455

Petitt P, Edwards ME, Forciniti D (1997) A small-angle neutron scattering study of gamma-crystallins near their isoelectric point. Eur Biophys J 243: 415–421

Rand RP (1992) Raising water to new heights. Science 256: 618

Record MT Jr, Anderson CF, Lohman TM (1978) Thermodynamic analysis of ion effects on the binding and conformational equilibria of proteins and nucleic acids: the roles of ion association or release, screening, and ion effects on water activity. Q Rev Biophys 11: 103–178

Rozhkov SP (1988) Spinodal in concentrated water-salt solutions of serum albumin molecules. Russ J Phys Chem 62: 1925–1929

Rozhkov SP (1992) Dependence of the sign of disjoining pressure in the hydration shell of a serum albumin molecule on the salt concentration: a spin-label evidence. Russ Colloid J 54: 64–69

Rozhkov SP (1996) Critical phenomena in water-salt solutions of biopolymers. Russ J Phys Chem 70: 1995–1999

Rozhkov SP (1997) Stabilization of albumin by the $CaCl_2$ and $MgCl_2$-regulated interaction of macromolecules: a spin-label study. Biophysics 42: 1033–1041

Rozhkov SP, Borisova AG (1993) Salt-induced phase-transition of the critical type in a water-protein matrix of serum albumin molecules. Biophysics 38: 590–545

Rupley JA, Carreri G (1991) Protein hydration and function. Adv Protein Chem 41: 137–172

Wasserman AM, Kovarskii AI (1986) Spin labels and probes in physical chemistry of polymers. Nauka, Moscow

Verheul M, Pedersen JS, Roefs SPFM, de Kruif KG (1999) Association behaviour of nature β-lactoglobulin. Biopolymers 49: 11–20

Wetzel R, Becker M, Behlke J, Billwitz H, Bohm S, Ebert B, Hamman H, Krubiegel J, Lassmann G (1980) Temperature behavior of human serum albumin. Eur J Biochem 104: 479–488